Absence of the nonpercolating phase for percolation on the nonplanar Hanoi network

Takehisa Hasegawa*
Graduate School of Information Sciences, Tohoku University, 6-3-09, Aramaki-Aza-Aoba, Sendai, 980-8579, Japan

Tomoaki Nogawa
Department of Mathematics, Tohoku University, 6-3-09, Aramaki-Aza-Aoba, Sendai, Miyagi 980-8579, Japan

(Received 21 December 2012; published 18 March 2013)

We investigate bond percolation on the nonplanar Hanoi network (HN-NP), which was studied previously [Boettcher *et al.* Phys. Rev. E **80**, 041115 (2009)]. We calculate the fractal exponent of a subgraph of the HN-NP, which gives a lower bound for the fractal exponent of the original graph. This lower bound leads to the conclusion that the original system does not have a nonpercolating phase, where only finite-size clusters exist for $p > 0$, or equivalently, that the system exhibits either the critical phase, where infinitely many infinite clusters exist, or the percolating phase, where a unique giant component exists. Monte Carlo simulations support our conjecture.

DOI: 10.1103/PhysRevE.87.032810 PACS number(s): 89.75.Hc, 64.60.aq, 89.65.−s

I. INTRODUCTION

Percolation is the simplest model exhibiting a phase transition [1]. Many results for percolation on Euclidean lattices have been reported. It is well known that bond percolation with open bond probability p on the $d(\geqslant 2)$-dimensional Euclidean lattice shows a second-order transition between the nonpercolating phase, where only finite-size clusters exist, and the percolating phase, where a unique giant component almost surely exists, at a unique critical point p_c. However, this may not be the case for non-Euclidean lattices.

Complex networks have been actively studied in recent years [2–4]. Among extensive researches carried out on complex networks, percolation on various networks has played an important role in clarifying the interplay between network topology and critical phenomena [5]. Percolation on uncorrelated networks (represented by the configuration model [6]) is well described by the local tree approximation; there is a phase transition between the nonpercolating phase and the percolating phase just as in Euclidean lattice systems, but its critical exponents depend crucially on the heterogeneity of the degree distribution of the network [7]. On the other hand, several authors [8–11] have reported that percolation on networks constructed with certain growth rules exhibits quite a different phase transition from that of uncorrelated networks and Euclidean lattices, referred to as an infinite-order transition with inverted Berezinskii-Kosterlitz-Thouless (BKT) singularity [12]: (i) The singularity of the phase transition is infinitely weak. When p lies above the transition point p_c, the order parameter $m(p) \equiv \lim_{N\to\infty} s_{\max}(N;p)/N$, where $s_{\max}(N;p)$ is the mean size of the largest cluster over percolation trials in the system with N nodes, obeys $m(p) \propto \exp[-\text{const.}/(\Delta p)^{\beta'}]$, where $\Delta p = p - p_c$. (ii) Below the transition point, the mean number n_s of clusters with size s per node obeys the power law $n_s \propto s^{-\tau}$. Furthermore, recent study [13] shows that a hierarchical small-world network exhibits a discontinuous transition instead of an infinite-order transition.

In [11,14,15], it has been found that for the growing network models the region below p_c corresponds to the critical phase (the intermediate phase), which has been observed in nonamenable graphs (NAGs) [16,17]. NAGs are defined to be transitive graphs with a positive Cheeger constant. Percolation on NAGs (with one end) exhibits the following three phases depending on the value of p: the nonpercolating phase ($0 \leqslant p < p_{c1}$), the critical phase ($p_{c1} < p < p_{c2}$), where infinitely many infinite clusters exist, and the percolating phase ($p_{c2} < p \leqslant 1$). Here, an infinite cluster is defined to be a cluster whose size is of order $O(N^\alpha)$ ($0 < \alpha \leqslant 1$). It is called a giant component when $\alpha = 1$. In the critical phase, where $0 < \alpha < 1$, the system is always in a critical state where n_s satisfies a power law [18].

All previous studies [8–11,14,15,19] of percolation on growing networks and hierarchical small-world networks indicate $0 = p_{c1} < p_{c2} < 1$, except in the following case. Boettcher *et al.* investigated bond percolation on the nonplanar Hanoi network (HN-NP) using the renormalization group technique [20]. They concluded that there are two critical probabilities p_{c1} and p_{c2} between zero and one: $0 < p_{c1} < p_{c2} < 1$.

In this paper, we reconsider this model. We show analytically that the fractal exponent of a subgraph, which is a lower bound for that of the HN-NP, takes a nonzero value at all $p(\neq 0)$, indicating that $p_{c1} = 0$. This means that the system is either in the critical phase or the percolating phase, not in the nonpercolating phase, in contrast to the result of [20]. The Monte Carlo simulations support our analytical prediction.

II. MODEL

The HN-NP consists of a one-dimensional chain and long-range edges. The HN-NP with $L(\geqslant 2)$ generation is constructed as follows [20]. (i) Consider a chain of $N_L = 2^L + 1$ nodes. Here, each node $i(=0,1,2,\ldots,N_L-1)$ connects to node $i+1$. We call these edges the *backbones*. (ii) For each combination of $i(=0,1,2,\ldots,L-2)$ and $j(=0,1,2,\ldots,2^{L-i-2}-1)$, nodes $(4j)2^i$ and $(4j+1)2^i$ are connected to $(4j+3)2^i$ and $(4j+4)2^i$, respectively. We call these edges the *shortcuts*. The schematic of the HN-NP with $L = 4$ generations is shown in Fig. 1. At generation L, the number of backbones is 2^L and the number of shortcuts is $2^L - 2$ (the total number of edges E_L is

*hasegawa@m.tohoku.ac.jp

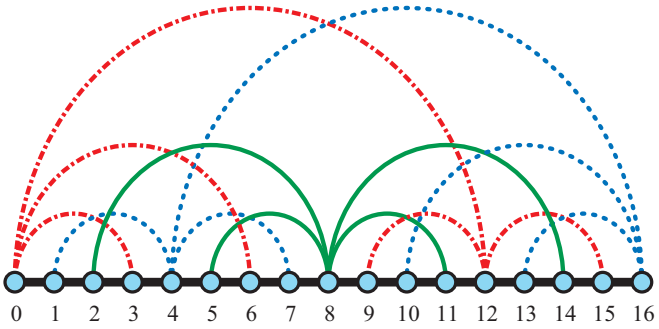

FIG. 1. (Color online) HN-NP with $L = 4$ generations. The black-thick lines are the backbones, and the red-dashed, green-solid, and blue-dotted lines are the shortcuts of the skeletons $T_a(4)$, $T_b(4)$, and $T_c(4)$, respectively.

$E_L = 2^{L+1} - 2$). The geometrical properties of the HN-NP are as follows [20]. (i) The degree distribution p_k decays exponentially as $p_{2m+3} \propto 2^{-m}$, (ii) the average degree $\langle k \rangle$ is $\langle k \rangle = 2E_L/N_L = (2^{L+2} - 4)/(2^L + 1) \approx 4$ (for $L \gg 1$), (iii) the mean shortest path length $\langle l \rangle$ increases logarithmically with N_L as $\langle l \rangle \propto \log N_L$, and (iv) the clustering coefficient is zero.

Boettcher *et al.* studied bond percolation on the HN-NP with open bond probability p [20]. In the HN-NP with L generations, they considered the renormalization of four parameters: R_L (the probability that three consecutive points a,b,c of a chain are connected), S_L (the probability of bc being connected, but not a), U_L (the probability of ac being connected, but not b), and N'_L (the probability that there are no connections among a, b, and c). From the renormalization group flow for R_L they determined the two critical probabilities as $p_{c1}^{\mathrm{BCZ}} \approx 0.319445$ and $p_{c2}^{\mathrm{BCZ}} \approx 0.381966$.

III. ANALYTICAL CALCULATION FOR THE SKELETON OF THE HN-NP

The fractal exponent $\psi_{\max}(p)$ is useful to determine phase behavior [18]. It is defined to be $\psi_{\max}(p) = \lim_{N_L \to \infty} \log_{N_L} s_{\max}(N_L; p)$. A nonpercolating phase, a critical phase, and a percolating phase are characterized by $\psi_{\max}(p) = 0$, $0 < \psi_{\max}(p) < 1$, and $\psi_{\max}(p) = 1$, respectively. Unfortunately, it seems difficult to evaluate $s_{\max}(N_L; p)$ directly for the HN-NP. Instead, we focus on a subgraph of the HN-NP and evaluate its fractal exponent.

We extract a subgraph from the HN-NP with L generations by removing the backbones. Because the resulting subgraph has no cycles and the number of shortcuts is $2^L - 2 = N_L - 3$, this subgraph is composed of three disconnected trees. Indeed, nodes $i = 0$, 2^{L-1}, and 2^L belong to the three different trees. We call these *the root nodes*. Here the graphs isomorphic to these trees and having root nodes $i = 0$, 2^{L-1}, and 2^L will be called the *skeletons* $T_a(L)$, $T_b(L)$, and $T_c(L)$, respectively. Clearly, $T_a(L)$ and $T_c(L)$ are also isomorphic to each other, $T_a(L) \simeq T_c(L)$. At $L = 2$, $T_a(2)$ is composed of nodes 0 and 3 and the edge between them, $T_b(2)$ is one isolated node $i = 2$, and $T_c(2)$ is composed of nodes 1 and 4 and the edge between them. The skeletons $T_a(L)$, $T_b(L)$, and $T_c(L)$ for arbitrary L are given recursively as follows. First, we consider two subgraphs of the sets of nodes $\{0,1,\ldots,2^{L-1}\}$ and $\{2^{L-1},2^{L-1}+1,\ldots,2^L\}$ after removing the backbones from the HN-NP with L generations. By symmetry, both subgraphs consist of the skeletons $T_a(L-1)$, $T_b(L-1)$, and $T_c(L-1)$ [Fig. 2(a)]. Here the root nodes of the latter subgraph are $i = 2^{L-1}$ [for $T_c(L-1)$], $3 \times 2^{L-2}$ [for $T_b(L-1)$], and 2^L [for $T_a(L-1)$]. Note that the skeletons $T_a(L)$, $T_b(L)$, and $T_c(L)$ are given by adding the two long-range edges $\{0,3 \times 2^{L-2}\}$ and $\{2^{L-2},2^L\}$, and taking into account the connection of node 2^{L-1} [Fig. 2(b)], we have

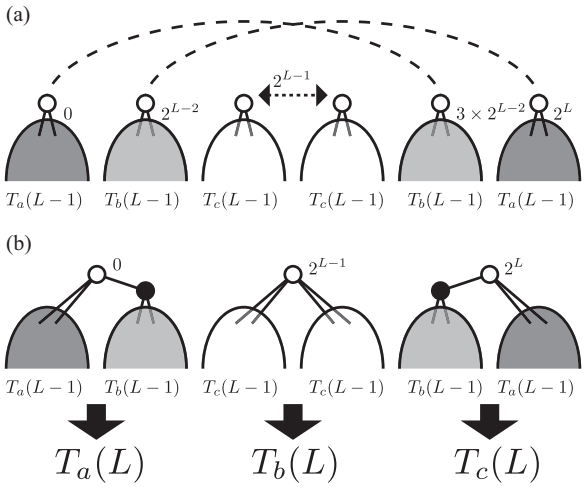

FIG. 2. Construction of the skeletons $T_a(L)$, $T_b(L)$, and $T_c(L)$. Open circles represent the root nodes of the skeletons.

$$T_a(L) \simeq T_c(L) \simeq R_1(T_a(L-1), T_b(L-1)), \quad (1)$$

$$T_b(L) \simeq R_2(T_c(L-1), T_c(L-1)), \quad (2)$$

where the operation $R_1(x,y)$ adds the edge between root nodes of the skeletons x and y, and $R_2(x,y)$ merges two root nodes of the skeletons x and y into one.

We now calculate the mean size of a cluster including the root node (the root cluster size) for each skeleton. We denote the root cluster sizes of $T_a(L)$ [$\simeq T_c(L)$] and $T_b(L)$ by $s_a(L)$ and $s_b(L)$, respectively. Because of the recursive structure [Eqs. (1) and (2)] of the skeletons, the root cluster sizes $s_a(L)$ and $s_b(L)$ also satisfy recursive relations:

$$s_a(L+1) = s_a(L) + p s_b(L), \quad (3)$$

$$s_b(L+1) = 2s_a(L) - 1, \quad (4)$$

where the initial conditions are $s_a(2) = 1 + p$ and $s_b(2) = 1$. Then, we find that

$$s_a(L) = \frac{1}{2} + \frac{(1+\sqrt{1+8p})^{L+1} - (1-\sqrt{1+8p})^{L+1}}{2^{L+2}\sqrt{1+8p}}, \quad (5)$$

$$s_b(L) = 1 + \frac{(1+\sqrt{1+8p})^{L} - (1-\sqrt{1+8p})^{L}}{2^{L}\sqrt{1+8p}}. \quad (6)$$

For $L \gg 1$, we obtain $s_a(L) \propto {N_L}^{\psi_{\mathrm{root}}^{\mathrm{skeleton}}(p)}$, where

$$\psi_{\mathrm{root}}^{\mathrm{skeleton}}(p) = \log_2(1+\sqrt{1+8p}) - 1. \quad (7)$$

We expect $\psi_{\mathrm{root}}^{\mathrm{skeleton}}(p) = \psi_{\mathrm{max}}^{\mathrm{skeleton}}(p)$ because the roots are hubs. In fact, we performed Monte Carlo simulations for the bond percolation on the skeletons. Our numerical result of

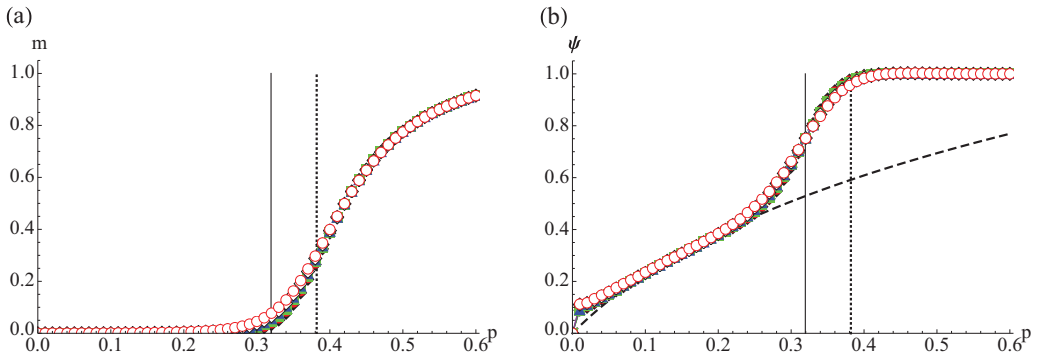

FIG. 3. (Color online) (a) Order parameter $m(N_L;p) = s_{\max}(N_L;p)/N_L$ and (b) fractal exponent $\psi(N_L;p)$. The numbers of generations L are 19 (black-diamond), 18 (red-circle), 17 (green-square), 16 (blue-triangle), 15 (open-diamond), and 14 (open-circle). The vertical solid line and dashed line indicate $p_{c1}^{\rm BCZ}$ and $p_{c2}^{\rm BCZ}$, respectively. In (b), the fractal exponent $\psi_{\rm root}^{\rm skeleton}(p)$ of the skeleton given by Eq. (7) is shown by the thick-dashed line.

$\psi_{\rm max}^{\rm skeleton}(p)$ shows a good correspondence with Eq. (7) except near $p = 0$ (not shown). According to Eq. (7), $\psi_{\rm root}^{\rm skeleton}(p)$ increases continuously from $\psi_{\rm root}^{\rm skeleton}(0) = 0$ to $\psi_{\rm root}^{\rm skeleton}(1) = 1$. This means that the subsystem consisting only of the shortcuts is in the critical phase for all $p(\neq 0,1)$, like the growing random tree [15]. Because the HN-NP is obtained by adding the backbones to the skeletons, the clusters in the skeletons become larger. Therefore, the entire system permits a critical phase even for infinitesimal p, i.e., the nonpercolating phase does not exist except at $p = 0$.

IV. NUMERICAL CHECK

In the previous section, we evaluated the root cluster size of the skeleton to show that its fractal exponent $\psi_{\rm root}^{\rm skeleton}(p)$ takes a nonzero value for all $p > 0$. Because the skeleton is just a subgraph of the HN-NP, $\psi_{\rm root}^{\rm skeleton}(p)$ is a lower bound for the fractal exponent of the largest cluster of the HN-NP $\psi_{\rm max}^{\rm HN-NP}(p)$, i.e., $\psi_{\rm root}^{\rm skeleton}(p) \approx \psi_{\rm max}^{\rm skeleton}(p) \leqslant \psi_{\rm max}^{\rm HN-NP}(p)$. For bond percolation on the HN-NP, $\psi_{\rm max}^{\rm HN-NP}(p) > 0$ when $p > 0$, implying that $p_{c1} = 0$. To check our prediction, we performed Monte Carlo simulations of bond percolation on the HN-NP. The number of generations is $L = 13, 14, \ldots, 20$, and the number of percolation trials is 100 000 for each p.

Figures 3(a) and 3(b) show the results for the order parameter $m(N_L;p)$ and the fractal exponent of the largest cluster $\psi_{\rm max}^{\rm HN-NP}(N_L;p)$, respectively. Here the fractal exponent $\psi_{\rm max}^{\rm HN-NP}(N_L;p)$ at a finite generation L is evaluated as

$$\psi_{\rm max}^{\rm HN-NP}(N_L;p) \approx \frac{\log s_{\max}(N_{L+1};p) - \log s_{\max}(N_{L-1};p)}{\log N_{L+1} - \log N_{L-1}}. \tag{8}$$

We also plot the fractal exponent $\psi_{\rm root}^{\rm skeleton}(p)$ of the skeleton [Eq. (7), shown as the thick-dashed line] and $p_{c1}^{\rm BCZ}$ and $p_{c2}^{\rm BCZ}$ (shown as vertical lines) in Fig. 3.

From Fig. 3(b), we see that $\psi_{\rm root}^{\rm skeleton}(p)$ is actually the lower bound of $\psi_{\rm max}^{\rm HN-NP}(p)$, implying that $p_{c1} = 0$. In particular, $\psi_{\rm max}^{\rm HN-NP}(N_L;p)$ coincides with $\psi_{\rm root}^{\rm skeleton}(p)$ for $p \lesssim 0.26$ (except near $p = 0$, where finite-size effects are not negligible). For $p \gtrsim 0.26$, $\psi_{\rm max}^{\rm HN-NP}(N_L;p)$ is considerably greater than $\psi_{\rm root}^{\rm skeleton}(p)$, and reaches unity at $p = p_{c2}^{\rm BCZ}$. At a glance, in the large-size limit, $\psi_{\rm max}^{\rm HN-NP}(N_L;p)$ seems to change continuously with $p < p_{c2}^{\rm BCZ}$. However, we speculate that in the large-size limit $\psi_{\rm max}^{\rm HN-NP}(N_L;p)$ (i) coincides with $\psi_{\rm root}^{\rm skeleton}(p)$ in the entire region below $p_{c1}^{\rm BCZ}$, (ii) jumps to a higher value at $p = p_{c1}^{\rm BCZ}$, and (iii) increases monotonically up to unity for $p_{c1}^{\rm BCZ} < p \leqslant p_{c2}^{\rm BCZ}$. The coincidence between $\psi_{\rm max}^{\rm HN-NP}(p)$ and $\psi_{\rm root}^{\rm skeleton}(p)$ for $p < p_{c1}^{\rm BCZ}$ means that the partial ordering [in the sense that the largest cluster is $O(N^{\alpha})$ with $\alpha < 1$]

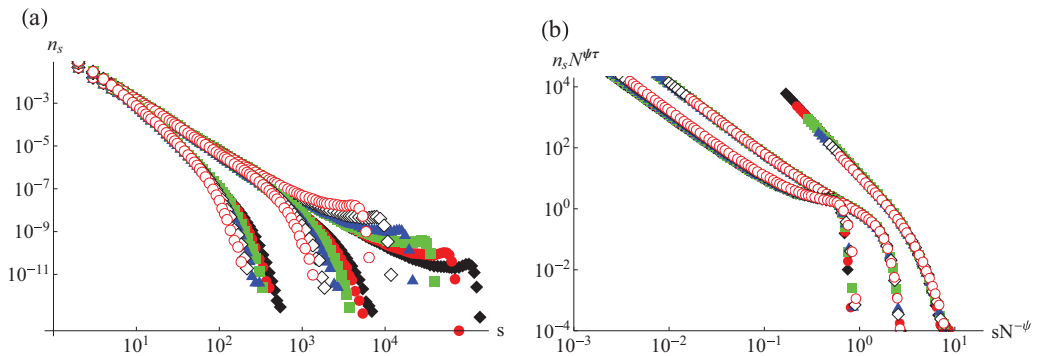

FIG. 4. (Color online) (a) Cluster size distribution $n_s(N_L;p)$ at $p = 0.16$, $0.26(< p_{c1}^{\rm BCZ})$, and $0.36(> p_{c1}^{\rm BCZ})$, from left to right. (b) Scaling result for $n_s(N_L;p)$ at $p = 0.20(< p_{c1}^{\rm BCZ})$, 0.32, and $0.35(> p_{c1}^{\rm BCZ})$, from right to left. The numbers of generations L are 19 (black-diamond), 18 (red-circle), 17 (green-square), 16 (blue-triangle), 15 (open-diamond), and 14 (open-circle).

in this region is essentially governed by the shortcuts. Because Boettcher *et al.* [20] considered renormalization of the connecting probability of consecutive points of the backbones, we would expect their first critical probability p_{c1}^{BCZ} to be the probability above which the backbones become relevant. Thus, we expect that there is a transition between critical phases, in the sense that the fractal exponent jumps, implying a qualitative change in the criticality, while it is very difficult to judge whether such a transition exists or not by finite-size simulations. Such a jump in the fractal exponent has already been observed in site-bond percolation on the decorated (2,2) flower [21]. In addition, our numerical result shows that $\psi_{\max}^{\mathrm{HN-NP}}(p)$ reaches unity smoothly at p_{c2}^{BCZ}. This indicates that the phase transition to the percolating phase is discontinuous, similarly as in [13].

Finally, we discuss the cluster size distribution function $n_s(p)$ below p_{c2}^{BCZ}. Figure 4(a) shows $n_s(p)$ for several values of p with $0 < p < p_{c2}^{\mathrm{BCZ}}$. In the critical phase, we expect a power law for $n_s(p)$:

$$n_s(p) \propto s^{-\tau(p)}, \tag{9}$$

where

$$\tau(p) = 1 + \psi_{\max}(p)^{-1}, \tag{10}$$

and a corresponding scaling form:

$$n_s(N_L; p) = N_L^{-\psi_{\max}(p)\tau(p)} f\left(s N_L^{-\psi_{\max}(p)}\right), \tag{11}$$

where the scaling function $f(\cdot)$ behaves as

$$f(x) \sim \begin{cases} \text{rapidly decaying func.} & \text{for} \quad x \gg 1, \\ x^{-\tau(p)} & \text{for} \quad x \ll 1. \end{cases} \tag{12}$$

We tested this scaling for $0 < p \lesssim 0.26$ and $p_{c1}^{\mathrm{BCZ}} < p < p_{c2}^{\mathrm{BCZ}}$ and obtained excellent collapses [Fig. 4(b)]. We would also expect n_s to be fat-tailed for $0.26 \lesssim p < p_{c1}^{\mathrm{BCZ}}$ because $n_s(p)$ for the skeletons perfectly obeys Eqs. (9) and (10) via Eq. (11) for $0 < p < 1$ (not shown), and n_s is broader when we add the backbones to the skeletons, i.e., for the original HN-NP.

V. SUMMARY

In this paper, we have studied bond percolation on the HN-NP. Our results give the two critical probabilities as $p_{c1} = 0 (< p_{c1}^{\mathrm{BCZ}})$ and $p_{c2} = p_{c2}^{\mathrm{BCZ}}$, implying that the system has only a critical phase and a percolating phase, and does not have a nonpercolating phase for $p > 0$. As far as we know, all complex network models with a critical phase have only the critical phase and the percolating phase ([8–11,13–15,19] for percolation and [12,19,22–27] for spin systems). It will be challenging to clarify the origin of such universal behavior.

ACKNOWLEDGMENT

T.H. acknowledges the support through Grant-in-Aid for Young Scientists (B) (No. 24740054) from MEXT, Japan.

[1] D. Stauffer and A. Aharony, *Introduction to Percolation Theory* (Taylor and Francis, London, 1994).
[2] R. Albert and A.-L. Barabási, Rev. Mod. Phys. **74**, 47 (2002).
[3] M. E. J. Newman, SIAM Rev. **45**, 167 (2003).
[4] A. Barrat, M. Barthélemy, and A. Vespignani, *Dynamical Processes on Complex Networks* (Cambridge University, Cambridge, England, 2008).
[5] S. N. Dorogovtsev, A. V. Goltsev, and J. F. F. Mendes, Rev. Mod. Phys. **80**, 1275 (2008).
[6] M. Molloy and B. Reed, Random Struct. Algor. **6**, 161 (1995).
[7] R. Cohen, D. ben-Avraham, and S. Havlin, Phys. Rev. E **66**, 036113 (2002).
[8] D. S. Callaway, J. E. Hopcroft, J. M. Kleinberg, M. E. J. Newman, and S. H. Strogatz, Phys. Rev. E **64**, 041902 (2001).
[9] S. N. Dorogovtsev, J. F. F. Mendes, and A. N. Samukhin, Phys. Rev. E **64**, 066110 (2001).
[10] L. Zalányi, G. Csárdi, T. Kiss, M. Lengyel, R. Warner, J. Tobochnik, and P. Érdi, Phys. Rev. E **68**, 066104 (2003).
[11] T. Hasegawa, M. Sato, and K. Nemoto, Phys. Rev. E **82**, 046101 (2010).
[12] M. Hinczewski and A. N. Berker, Phys. Rev. E **73**, 066126 (2006).
[13] S. Boettcher, V. Singh, and R. M. Ziff, Nature Commun. **3**, 787 (2012).
[14] T. Hasegawa, T. Nogawa, and K. Nemoto, arXiv:1009.6009.
[15] T. Hasegawa and K. Nemoto, Phys. Rev. E **81**, 051105 (2010).
[16] I. Benjamini and O. Schramm, Electron. Comm. Probab. **1**, 71 (1996).
[17] R. Lyons, J. Math. Phys. **41**, 1099 (2000).
[18] T. Nogawa and T. Hasegawa, J. Phys. A: Math. Theor. **42**, 145001 (2009).
[19] A. N. Berker, M. Hinczewski, and R. R. Netz, Phys. Rev. E **80**, 041118 (2009).
[20] S. Boettcher, J. L. Cook, and R. M. Ziff, Phys. Rev. E **80**, 041115 (2009).
[21] T. Hasegawa, M. Sato, and K. Nemoto, Phys. Rev. E **85**, 017101 (2012).
[22] M. Bauer, S. Coulomb, and S. N. Dorogovtsev, Phys. Rev. Lett. **94**, 200602 (2005).
[23] E. Khajeh, S. N. Dorogovtsev, and J. F. F. Mendes, Phys. Rev. E **75**, 041112 (2007).
[24] S. Boettcher and C. T. Brunson, Phys. Rev. E **83**, 021103 (2011).
[25] S. Boettcher and C. Brunson, Front. Physiol. **2**, 102 (2011).
[26] T. Nogawa, T. Hasegawa, and K. Nemoto, Phys. Rev. Lett. **108**, 255703 (2012).
[27] T. Nogawa, T. Hasegawa, and K. Nemoto, Phys. Rev. E **86**, 030102 (2012).